Terms linear in k in the band structure of wurtzite-type semiconductors

L. C. Lew Yan Voon, M. Willatzen, and M. Cardona
Max-Planck-Institut für Festkörperforschung, Heisenbergstraße 1, D-70569 Stuttgart, Germany

N. E. Christensen
Institute of Physics and Astronomy, University of Aarhus, DK-8000 Aarhus C, Denmark
(Received 14 June 1995; revised manuscipt received 3 November 1995)

Wurtzite has the space-group symmetry $P6_3mc$. The absence of inversion symmetry allows linear-k terms in the electronic band structure when the spin-orbit interaction is included. Their existence has been confirmed in a number of experiments, but no microscopic calculations have been published. In the present paper, we discuss the origin of these linear-k terms using group theory and $\mathbf{k}\cdot\mathbf{p}$ arguments. The various contributions to these terms are identified through band-structure models. We present an *ab initio* calculation, performed with the linear-muffin-tin-orbital method, of these spin splittings in CdS, CdSe, and ZnO. A renormalization of the valence-band spin-splitting coefficients obtained in the linear-muffin-tin-orbital calculations was found necessary to correct for errors in the relative energies of the uppermost valence bands as compared with the experimental values. We point out that a similar procedure should be used when evaluating masses and other band parameters from calculated local-density-approximation band structures.

I. INTRODUCTION

The band structures of zinc-blende and wurtzite-type compound semiconductors are nondegenerate at a general $\mathbf{k}$ point of the Brillouin zone (BZ).[1,2] The corresponding splittings of spin-degenerate states arise from the lack of inversion symmetry through the action of the spin-orbit coupling. At the Γ point of the BZ these energy splittings vanish. They can be expanded around Γ in linear, cubic, and other odd terms in k. The corresponding coefficients can be determined by means of a variety of mostly optical experiments. They account for a number of sophisticated phenomena as diverse as the width of spin-flip Brillouin lines,[3] the spin-relaxation in luminescence[4] and photoemission excited with linearly polarized light,[5] and confinement effects in nanocrystals imbedded in a matrix.[6] Recent interest has concentrated in phenomena related to spin splittings in quantum wells whose understanding is based on the corresponding effects in bulk materials.[7–9] Such understanding is available for zinc-blende-type[10] but not for wurtzite-type semiconductors. The materials with wurtzite structure, CdS, CdSe, and ZnO, are the object of the present work.

Two types of linear-k terms are possible in the band structure near the Γ point. One results from the splitting of spin-degenerate doublets, while the other is a linear splitting between states which remain spin-degenerate. We note that both are allowed for a zinc-blende crystal (for example, at the top of the valence band, along the $\langle 111\rangle$ and $\langle 100\rangle$ directions, respectively[1]). The second possibility requires a minimum fourfold degeneracy. While such degeneracy may exist in zinc blende, it is reduced in wurtzite to twofold by the hexagonal crystal field: The combination of crystal-field and spin-orbit energies leads to a three-edge structure involving the top of the valence band known as the A, B, and C edges in order of increasing energy. The corresponding excitons are similarly labeled. Two of these three edges are of Γ_7 and one of Γ_9 symmetry, while the lowest conduction state has Γ_7 symmetry. The valence states are, in order of decreasing energy, Γ_9, Γ_7, and Γ_7 for CdS and CdSe; we call this the normal ordering.[11,12] In ZnO the ordering is Γ_7-Γ_9-Γ_7. This *anomalous* ordering results from a negative spin-orbit splitting.[13]

The existence and influence of the linear-k terms for wurtzite has been vigorously investigated since the 1950s.[2,11,12,14–24] Such a flurry of activity was initially mainly due to the simpler exciton structure, compared to the zinc-blende case, and the easy accessibility of the absorption edge of CdS ($\sim$ 2.5 eV) to spectroscopic sources. More recent interest was sparked by the proposal of Brenig, Zeyher, and Birman[25] that resonant Brillouin scattering could be used to decide among the various additional boundary conditions (the ABC problem[26]) for light propagation across the interface of a crystal displaying spatial dispersion.[27–30] The linear-k terms in the excitonic dispersion lead to a multimode polariton dispersion. A summary of the bulk zinc-blende work up to 1988 is available in Ref. 31. Recent interest has focused on linear spin splittings in zinc-blende materials induced by quantum confinement.[7,9,32,33]

It is known that the Γ_9 states of wurtzite are not linearly spin split.[16,21] Hopfield[19] estimated the upper limits for the linear splittings of the conduction (e) and B-valence Γ_7 states of CdS and CdSe to be[34]

	e (CdS)	B (CdS)	e (CdSe)	B (CdSe)
C (meVÅ)	6	600	100	900

Subsequently, Mahan and Hopfield[21] used the spatial-dispersion of excitons in order to explain the presence of an ''anomalous'' structure in the reflection spectra near the B-exciton resonance. They extracted a value of 50 meV Å for the linear spin-splitting coefficient of the B exciton of CdS. Hopfield and Thomas[20] also showed that the exciton-polariton dispersion relation is strongly modified by the pres-

ence of the linear-k terms. This theory has been the basis for the analysis of recent experiments, a number of which have focused on the determination of the linear-splitting coefficients of the A and B excitons of both CdS and ZnO.[22,27–30] The analysis, however, involves a number of additional parameters (e.g., exciton masses, exciton energies, damping constants, etc.). There appears to be only one direct determination of the linear spin-splitting coefficient of a band edge (as opposed to that of an exciton), namely the conduction-band spin-flip Raman scattering work of Romestain *et al.*[3] No determination of the C_i's for CdSe has been carried out, beyond the work of Hopfield mentioned above. Finally, no data are available for the C valence state.

In this paper, we discuss the requirements for the presence of such linear-k terms in wurtzite crystals and calculate their magnitudes. We address the following questions: how do the linear spin-splitting coefficients for wurtzite crystals compare with those for zinc-blende crystals and can the atomic-sphere-approximation linear-muffin-tin-orbital (ASA-LMTO) method, so successfully used to calculate the linear and cubic spin-splitting coefficients of zinc-blende crystals,[10,31] predict the linear coefficients for wurtzite crystals? We start with group-theory and $\mathbf{k}\cdot\mathbf{p}$ arguments (Sec. II). We then present in Sec. III results of *ab initio* calculations for these terms based on the ASA-LMTO method. Uncorrected and band-gap-corrected local-density approximation calculations allow us to confirm the qualitative correctness of our $\mathbf{k}\cdot\mathbf{p}$ model. To our knowledge, no *ab initio* calculated values for any of the C_i's are found in the literature. Our calculations agree with experimental values. For completeness, a comparison of the spin splittings in wurtzite and zinc-blende CdSe is presented.

II. LINEAR-k FORMALISM

The combination of spatial inversion asymmetry and the spin-orbit term in the electronic Hamiltonian leads to spin-split energy bands.[1,2,35] The spin-orbit interaction removes what would otherwise be a degeneracy of spin-up and spin-down states. Similarly, under inversion asymmetry no additional degeneracy appears at a general point of the BZ other than the Kramers degeneracy between $\psi_\uparrow(\mathbf{k})$ and $T\psi_\uparrow(\mathbf{k})$ $[=\psi_\downarrow(-\mathbf{k})]$, where T is the time-reversal operator: for $k=0$, one thus recovers a minimum double degeneracy. The resulting spin splitting is odd in $\mathbf{k}$.

For zinc-blende, the first s-like conduction state displays no linear splitting. On the other hand, the topmost p-like valence states can display small linear splittings mainly due to coupling to d-like core states. This is best shown through a perturbative analysis of the $\mathbf{k}\cdot\mathbf{p}$ Hamiltonian:[31,35]

$$H(\mathbf{k})=H(0)+\frac{\hbar^2k^2}{2m_0}+\frac{\hbar}{m_0}\mathbf{k}\cdot\mathbf{p}+H_1+H_2, \tag{1}$$

where

$$H_1=\frac{\hbar^2}{4m_0^2c^2}[\nabla V\times\mathbf{k}]\cdot\boldsymbol{\sigma}, \quad H_2=\frac{\hbar}{4m_0^2c^2}[\nabla V\times\mathbf{p}]\cdot\boldsymbol{\sigma}. \tag{2}$$

Cubic terms arise from fourth-order perturbation theory (three times $\mathbf{k}\cdot\mathbf{p}$ plus one time H_2), while linear-k terms arise from either first-order (H_1) or second-order (H_2 and $\mathbf{k}\cdot\mathbf{p}$) perturbation theory. Hence, very near Γ, a nonvanishing linear splitting will generally dominate. We now discuss its existence in the wurtzite structure.

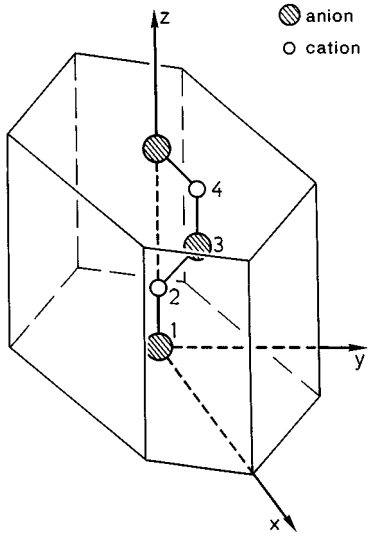

FIG. 1. Wurtzite primitive cell. The coordinates of the four atoms are $\mathbf{t}_1=(0,0,0)$, $\mathbf{t}_2=(0,0,uc)$, $\mathbf{t}_3=(0,a/\sqrt{3},c/2)$, $\mathbf{t}_4=(0,a/\sqrt{3},c/2+uc)$.

A. Symmetry considerations

In real space, the primitive cell of the wurtzite crystal is a hexagonal prism with four atoms (Fig. 1). It is characterized by three lattice parameters: the length of the c axis, the c/a ratio, and the bond-length parameter u. The corresponding BZ is also a hexagonal prism (Fig. 2). The labeling of the high-symmetry points and lines follows Refs. 2 and 36.

At the BZ center and along the Γ-A direction, the group of $\mathbf{k}$ ($\mathcal{G}_\mathbf{k}$) is C_{6v}, and the irreducible representations compatible with spin are the doubly-degenerate Γ_7, Γ_8, and Γ_9 (Table I). There is, therefore, no spin splitting along the

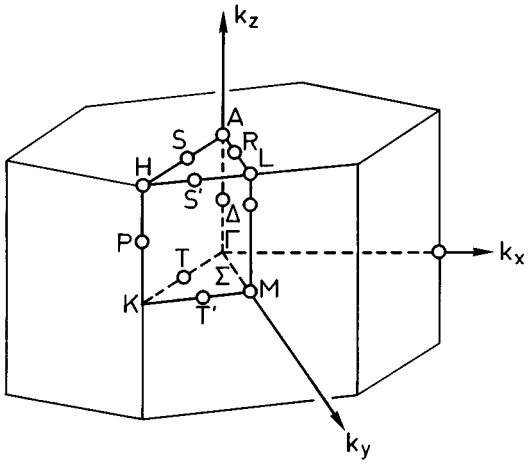

FIG. 2. Brillouin zone of a wurtzite crystal. The coordinates of some points are $A=2\pi(0,0,1/2c)$, $L=2\pi(0,1/\sqrt{3}a,1/2c)$, $M=2\pi(0,1/\sqrt{3}a,0)$, $H=2\pi(-1/3a,1/\sqrt{3}a,1/2c)$, $K=2\pi(-1/3a,1/\sqrt{3}a,0)$.

TABLE I. Character table for the double group of $\mathbf{k}$ C_{6v} $(6mm)$ at the zone center (Γ point) of the BZ for the wurtzite crystal structure and corresponding basis functions. Adapted from Koster *et al.* (Ref. 53).

C_{6v}	E	C_2	$2C_3$	$2C_6$	$3\sigma_v$	$3\sigma_d$		Basis	
Γ_1	1	1	1	1	1	1		$s,z,3z^2-r^2$	
Γ_2	1	1	1	1	-1	-1		R_z	
Γ_3	1	-1	1	-1	-1	1		x^3-3xy^2	
Γ_4	1	-1	1	-1	1	-1		y^3-3yx^2	
Γ_5	2	-2	-1	1	0	0		$(R_x,R_y),(x,y),(zx,yz)$	
Γ_6	2	2	-1	-1	0	0		(x^2-y^2,xy)	
	E	$\overline{E}$	$C_2,\overline{C}_2$	$2C_3$	$2\overline{C}_3$	$2C_6$	$2\overline{C}_6$	$3\sigma_v,3\overline{\sigma}_v$	$3\sigma_d,3\overline{\sigma}_d$
Γ_7	2	-2	0	1	-1	$\sqrt{3}$	$-\sqrt{3}$	0	0
Γ_8	2	-2	0	1	-1	$-\sqrt{3}$	$\sqrt{3}$	0	0
Γ_9	2	-2	0	-2	2	0	0	0	0

hexagonal axis. The highest symmetry for an internal BZ point (i.e., excluding the origin and zone-edge) is C_s (along, for example, the T direction) and all the irreducible representations compatible with spin are singly degenerate. Hence, except for accidental or time-reversal degeneracy, spin splittings must occur for all bands. It remains to determine whether the splitting is linear in k or of higher order. The existence and general form of the linear (or, similarly, higher-order) spin-splitting Hamiltonian can be deduced immediately by noting that the effective spin Hamiltonian is an invariant (with respect to $\mathcal{G}_{\mathbf{k}}$) linear in the components of the wave vector $\mathbf{k}$. With the help of Table I, one can then write this invariant as

$$H \propto [\sigma_x k_y - \sigma_y k_x], \tag{3}$$

since (k_x,k_y) and (σ_x,σ_y) both belong to Γ_5.[19]

We discuss next the mixing of states with atomiclike s, p, and d character at Γ in a wurtzite crystal. Without spin all states transform according to one of the single-group representations of C_{6v}, as given in Table I. In particular,

$$s,p_z,d_{3z^2-r^2} \sim \Gamma_1, \quad (p_x,p_y),(d_{zx},d_{yz}) \sim \Gamma_5,$$

$$(d_{x^2-y^2},d_{xy}) \sim \Gamma_6. \tag{4}$$

Contrary to the cubic case, the three p-like functions no longer belong to the same irreducible representation. Furthermore s, p_z, and $d_{3z^2-r^2}$ mixing is now allowed. When spin is introduced, one obtains the double-group representations:

$$\Gamma_1 \rightarrow \Gamma_7, \quad \Gamma_5 \rightarrow \Gamma_7 \oplus \Gamma_9, \quad \Gamma_6 \rightarrow \Gamma_8 \oplus \Gamma_9. \tag{5}$$

The influence of the crystal field and spin-orbit interaction is sketched in Fig. 3.

B. k·p theory

Equation (1) provides the basis for investigating the existence and origin of spin-splitting terms to various orders in k through perturbation theory. Linear terms in k can arise from two possible contributions: either through H_1 as a first-order perturbation, or through a second-order perturbation involving $\mathbf{k}\cdot\mathbf{p}$ and H_2, leading to the matrix

$$\frac{\hbar}{m_0}\sum_{\overline{L}\neq L} \frac{\langle L|H_2|\overline{L}\rangle\langle\overline{L}|\mathbf{k}\cdot\mathbf{p}|L\rangle + \langle L|\mathbf{k}\cdot\mathbf{p}|\overline{L}\rangle\langle\overline{L}|H_2|L\rangle}{E_L - E_{\overline{L}}}, \tag{6}$$

where L corresponds to the unperturbed degenerate set of states.

1. Γ-point eigenstates

To calculate the spin splitting of the e, A, B, and C states very near the Γ point, explicit wave functions at the Γ point are required. The latter are more complicated than for the zinc-blende case [see Eq. (4)]. Nevertheless, the following qualitative picture applies: e is mostly s-like with some p_z character, while the A, B, and C states are predominantly p-like with some d character and, in the case of the Γ_7 states, some s-character.

The relative separation of the e state from the valence states ($\sim$3 eV compared to $\sim$0.1–0.5 eV for the A–C separation) allows us to make a simplifying approximation. We first mix the s and p_z functions and then solve the valence Hamiltonian separately. We will see later that the s-p_z mixing is indeed important in interpreting the linear spin-splitting coefficients for both the conduction and valence states. Hence, for the e state, we write

$$|S\rangle = q_s|s\rangle + q_z|z\rangle, \quad \ni q_s^2 + q_z^2 = 1, \tag{7}$$

and, for the Γ_{1v} state,

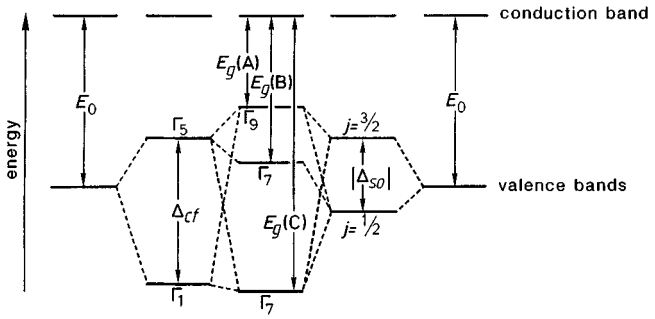

FIG. 3. Band mixing under the action of crystal-field and spin-orbit interactions in wurtzite crystals. To the left, splitting induced only by the crystal field; to the right, splitting induced only by the spin-orbit interaction. The combined case is given in the middle.

$$|Z\rangle = q_z'|z\rangle + q_s'|s\rangle, \quad q_z' = q_s, q_s' = -q_z. \tag{8}$$

It is now necessary to diagonalize the valence Hamiltonian exactly. A popular set of solutions is obtained by approximating the wurtzite crystal by a zinc-blende one strained along the [111] direction (the so-called quasicubic model[17]). We here use, instead, the more general valence-band solutions of Gutsche and Jahne.[37] They go beyond the quasicubic model keeping the correct symmetry of the wurtzite crystal with all its anisotropies, including d-like functions into the Γ_9 states. Cellular functions transforming according to the Γ_1, Γ_3, Γ_5, and Γ_6 single-group representations were used as basis functions (see Table I):

$$u_1 = Z, \quad u_3 = x(x^2 - 3y^2), \quad u_5 = (x + iy)/\sqrt{2},$$

and

$$u_6 = (x + iy)^2/2. \tag{9}$$

We here reproduce, with slight modifications, the Γ_7 and Γ_9 solutions of Ref. 37:

$$|\Gamma_7\uparrow\rangle = \sqrt{1-q_7^2}|u_5\downarrow\rangle - q_7|u_1\uparrow\rangle,$$

$$|\Gamma_9\uparrow\rangle = \sqrt{1-q_9^2}|u_5\uparrow\rangle + q_9|u_6\downarrow\rangle,$$

$$|\Gamma_7\downarrow\rangle = -\sqrt{1-q_7^2}|u_5^*\uparrow\rangle - q_7|u_1\downarrow\rangle,$$

$$|\Gamma_9\downarrow\rangle = \sqrt{1-q_9^2}|u_5^*\downarrow\rangle - q_9|u_6^*\uparrow\rangle,$$

$$|\Gamma_{7'}\uparrow\rangle = q_7|u_5\downarrow\rangle + \sqrt{1-q_7^2}|u_1\uparrow\rangle,$$

$$|\Gamma_{9'}\uparrow\rangle = -q_9|u_5\uparrow\rangle + \sqrt{1-q_9^2}|u_6\downarrow\rangle,$$

$$|\Gamma_{7'}\downarrow\rangle = -q_7|u_5^*\uparrow\rangle + \sqrt{1-q_7^2}|u_1\downarrow\rangle,$$

$$|\Gamma_{9'}\downarrow\rangle = -q_9|u_5^*\downarrow\rangle - \sqrt{1-q_9^2}|u_6^*\uparrow\rangle, \tag{10}$$

where the q_i's are cellular-function-mixing constants.[37] For CdS the A state has predominantly (x,y) character with some d state admixture. We choose A to correspond to Γ_9 ($m_j = \pm 3/2$), i.e., to the small q_9 limit. The $\Gamma_{9'}$ state has then predominant d character and is therefore known from experiments not to be one of the A, B, C states. The B state is mainly z-like with some (x,y) and s mixed in, and vice versa for the C state. Following Ref. 38 we choose $q_7^2 > 0.5$; this implies that $B \sim \Gamma_7$ and $C \sim \Gamma_{7'}$ (both having $m_j = \pm 1/2$). The zinc-blende limit is obtained for $q_7^2 = 2/3$.

We now combine each state of a given symmetry with its Kramers degenerate partner (uniquely defined by $Tu_i\uparrow = u_i^*\downarrow, Tu_i\downarrow = -u_i^*\uparrow$) and generate a 2×2 spin matrix with off-diagonal matrix elements linear in $\mathbf{k}$. We obtain [see Eq. (3)]

$$H_m(\mathbf{k}) = C_m \begin{bmatrix} 0 & ik_- \\ -ik_+ & 0 \end{bmatrix}, \tag{11}$$

where $k_\pm = k_x \pm ik_y$, C_m is labeled with the band edge Γ_m, and the band-edge energies have been set to zero. The linear-k splitting resulting from Eq. (11) is isotropic in the plane perpendicular to the hexagonal axis:

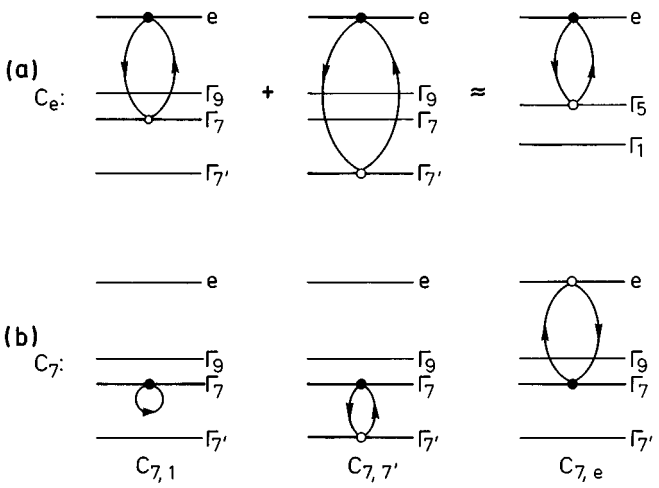

FIG. 4. Perturbation theory diagrams for the linear-k spin-splitting coefficients (a) of the e state, (b) of the Γ_{7v}. In (a), the double-group diagrams (left) add up approximately to give the single-group diagram (right).

$$E_m(k_x, k_y) = \pm C_m(k_x^2 + k_y^2)^{1/2}. \tag{12}$$

We assume that most of the contributions to the linear-k splittings of the e, A, B, and C states can be accounted for by intraband and interband interactions involving only these bands (hereafter referred to as the $eABC$ model). This should be a good approximation since the other states are indeed relatively far away in energy. The more general results, which include interactions among all the Γ_7-like states, are given in the Appendix.

2. H_1 and H_2 perturbations for the e state

The H_1 contribution would be

$$C_{e,1} \propto \langle S|\nabla_z V|S\rangle. \tag{13}$$

Since $|S\rangle$ is a solution of the Hamiltonian without the spin-orbit terms, one finds[31]

$$\langle S|\nabla_z V|S\rangle \propto \langle S|[H(0), p_z]|S\rangle = 0. \tag{14}$$

Within the $eABC$ model, one has

$$C_e = C_{e,7} + C_{e,7'}, \tag{15}$$

where $C_{e,7}$ ($C_{e,7'}$) denotes the contribution of the Γ_7 ($\Gamma_{7'}$) state to C_e, with

$$C_{e,7} = \frac{(1-q_7^2)}{E_e - E_7} q_z q_s \Delta_{x,z} P_{x,s},$$

$$C_{e,7'} = \frac{q_7^2}{E_e - E_{7'}} q_z q_s \Delta_{x,z} P_{x,s}. \tag{16}$$

Equations (15) and (16) are depicted schematically in Fig. 4(a). Note that $C_{e,7}$ and $C_{e,7'}$ have the same sign and C_e would be zero if there were no s-p_z mixing ($q_z = 0$). Knowing q_7 and the band-edge energies allows an explicit determination of the contribution of each of the B and C edges (in the normal-ordering case) to C_e; a simplified expression can

be obtained if one approximates the two energy denominators by a single average-gap energy E_5:

$$C_e \approx q_z q_s \frac{\Delta_{x,z}}{E_e - E_5} P_{x,s}. \tag{17}$$

This result is independent of q_7. Since the s-p_z mixing factor q_z is roughly inversely proportional to the energy gap, one expects

$$C_e \propto \frac{1}{(E_e - E_5)^2}. \tag{18}$$

The simple form of Eq. (17) allows one to infer the sign of the spin-splitting coefficient for the e band and estimate its magnitude. As in the case of zinc-blende semiconductors,[10,31,39] the sign is only meaningful if one chooses a convention for the split-level ordering and a specific orientation of the bonds with respect to the crystal axes. Since the sign of the C_i's has not been discussed in the literature (the experimental assignment being nontrivial), we conjecture the following. We make use of the fact that the nearest-neighbor environments for zinc-blende and wurtzite are similar. Paralleling the convention made in Refs. 10 and 39 for zinc-blende, we place the anions and cations as shown in Fig. 1. This allows us to carry over to wurtzite the following zinc-blende result: $-i\Delta_{z,x} > 0$, $iP_{x,s} > 0$. While this applies to CdS and CdSe, we expect the negative spin-orbit energy of ZnO to lead to $-i\Delta_{z,x} < 0$. The signs of q_s and q_z in Eq. (15) are trickier. The zinc-blende symmetry gives a net cancellation of s-p_z mixing from the four nearest neighbors at $k=0$. Obviously, deviations from this ''ideal'' tetrahedral geometry will lead to a net mixing, but this effect is expected to be small. The second-nearest-neighbor Cd-S interactions are found to be more important. One can then show that, irrespective of the phase chosen for the s orbital on the anion at the origin, $q_s q_z < 0$. Finally, because of the assumption made above, of all the Γ_5 states the main contribution arises from the one nearest to the e state, i.e., the top of the valence band in the absence of the spin-orbit interaction; thus, $E_e > E_5$. This leads to $C_e > 0$ in Eq. (11) for wurtzite semiconductors with normal ordering. This implies, using Eq. (11), that along the $+k_x$ direction, the state with up-spin has higher energy than the one with down-spin. An assignment of C_e positive implies that, looking along the $+k_z$ axis, the positive spin eigenstate appears to rotate clockwise. From Eq. (17), one can also estimate the magnitude of the linear spin-splitting coefficient of the e state. Using the III-V zinc-blende value of $P \sim 0.6$ a.u., the sulfur spin-orbit energy ~ 0.1 eV, 2% p_z wave-function mixing (obtained from our LMTO calculations below), and the band gap of ~ 2.5 eV, one obtains $C_e \sim 30$ meV Å. A similar analysis in Ref. 19 yielded $C_e \sim 6$ meV Å.

3. H_1 and H_2 perturbations for Γ_7 valence states

Consider first the H_1 perturbation [Fig. 4(b), left]. In this case, using Eq. (10),

$$C_{7,1} = -C_{7',1} = \frac{\sqrt{2}\hbar^2}{4m_0^2c^2} q_7 (1-q_7^2)^{1/2} \left\langle x \left| \frac{\partial V}{\partial x} \right| Z \right\rangle. \tag{19}$$

TABLE II. Adjusting-potential [V_0, Eq. (25)] and atomic-sphere parameters for the ASA-LMTO calculations for CdS. $E1$ and $E2$ are the two types of empty spheres. Energies are given in hartree (27.2 eV) and distances in bohr.

	Cd	S	$E1$	$E2$
V_0 (hartree)	750.0	50.0	7.5	7.5
R_0 (a.u.)	0.015	0.015	0.55	0.55
atomic radius (a.u.)	2.72	2.72	2.176	3.105

For the H_1 contribution, one would then expect equal and opposite spin splitting for the B and C states of either CdS or CdSe, and for the A and C states of ZnO. In addition, it should not depend strongly on the band gap. Gutsche and Jahne[37] have estimated $q_7^2 \sim 0.43, 0.6$, and 0.01 for CdS, CdSe, and ZnO, respectively.

We next turn to the H_2 contribution to the linear spin splitting. In fact, this contribution has been found, for the zinc-blende semiconductors, to be more important than that of H_1.[31] General expressions are given by Eqs. (A6) and (A7). They also simplify considerably if one restricts oneself to the $eABC$ model. In this case, Γ_{7v} ($\Gamma_{7v'}$) couples directly with e and $\Gamma_{7v'}$ (Γ_{7v}). Thus, in Eq. (A6) [Eq. (A7)], the first (second) term on the right-hand side should be removed. The explicit results for Γ_{7v} are

$$C_{7v} = C_{7,e} + C_{7,7'}, \tag{20}$$

with

$$C_{7,e} = -C_{e,7},$$

$$C_{7,7'} = \frac{1}{\sqrt{2}} q_s' \frac{(1-2q_7^2)}{(E_7 - E_{7'})} P_{x,s} [-q_7 (1-q_7^2)^{1/2} \Delta_{x,y} + \sqrt{2} q_z' (1-2q_7^2) \Delta_{x,z}]. \tag{21}$$

For $\Gamma_{7'v}$, we obtain an overall sign change; i.e.,

$$C_{7'v} = C_{7',e} + C_{7',7} = -C_{7,2}, \ni C_{7',e} = -C_{7,e}$$

and

$$C_{7',7} = -C_{7,7'}. \tag{22}$$

In words, the $\Gamma_7 - \Gamma_{7'}$ interaction [Fig. 4(b), middle] is equal and opposite for the Γ_7 and $\Gamma_{7'}$ states *and* arises due to the mixing of s-like states into the Γ_7 state and $\Gamma_{7'}$ states (q_s'). The magnitude of $C_{7,7'}$ can also be seen from Eqs. (21) and (16) to satisfy

$$|C_{7,7'}| = |C_{7',7}| \propto \frac{1}{(E_7 - E_{7'})(E_e - E_5)} \sim \left| \frac{(E_e - E_5)}{(E_7 - E_{7'})} C_e \right|. \tag{23}$$

The $\Gamma_7 - \Gamma_e$ interaction [Fig. 4(b), right] is the same as in C_e except for the opposite sign.

The various contributions to the spin-splitting coefficients can thus be written as

TABLE III. Lattice parameters used in the ASA-LMTO calculations for wurtzite CdS, CdSe, and ZnO. We used experimental values of a and c, and the ideal value of the (internal) lattice parameter u. We have also tabulated reported experimental and calculated values for u (last two rows, respectively).

	CdS	CdSe	ZnO
a	4.14092[a]	4.300[b]	3.24982[c]
c	6.7198[a]	7.011[b]	5.20661[c]
c/a	1.6228	1.630	1.6021
u	0.3766[d]	0.3754[d]	0.3799[d]
	0.3773[e]	0.3767[e]	0.3820[e]
	0.3728[f]	0.3700[f]	0.3793[f]

[a]N. Razik, J. Mater. Sci. Lett. **6**, 1443 (1987)
[b]Nat. Bur. Stand. Circ. 5397, 12 (1957).
[c]Nat. Bur. Stand. (US) Monograph **22** (1985).
[d]"Ideal" values [Eq. (26)] using the experimental c/a values.
[e]H. Schulz and K. H. Thiemann, Solid State Commun. **32**, 783 (1979).
[f]Theory (present work): total-energy minimization using the full-potential LMTO method.

$$C_e \sim \left[\frac{(1-q_7^2)}{E_e-E_7}+\frac{q_7^2}{E_e-E_{7'}}\right]\frac{\mathscr{A}}{(E_e-E_5)},$$

$$C_7 \sim -\frac{(1-q_7^2)}{(E_e-E_7)}\frac{\mathscr{A}}{(E_e-E_5)}+\frac{\mathscr{B}}{(E_7-E_{7'})(E_e-E_5)}+\mathscr{C}, \tag{24}$$

$$C_{7'} \sim -\frac{q_7^2}{(E_e-E_7)}\frac{\mathscr{A}}{(E_e-E_5)}-\frac{\mathscr{B}}{(E_7-E_{7'})(E_e-E_5)}-\mathscr{C},$$

where $\mathscr{A}$, $\mathscr{B}$, and $\mathscr{C}$ stand for coefficients which should be approximately independent of the band-edge energies. The sign of $\mathscr{A}$ for semiconductors with normal ordering of the valence states has been assigned above (>0); the term containing $\mathscr{B}$ (in C_7 and $C_{7'}$) is expected to be the largest one and that containing $\mathscr{C}$ the smallest in magnitude. The Γ_{9v} state does not appear in Eq. (24). These equations will be used in interpreting the LMTO results.

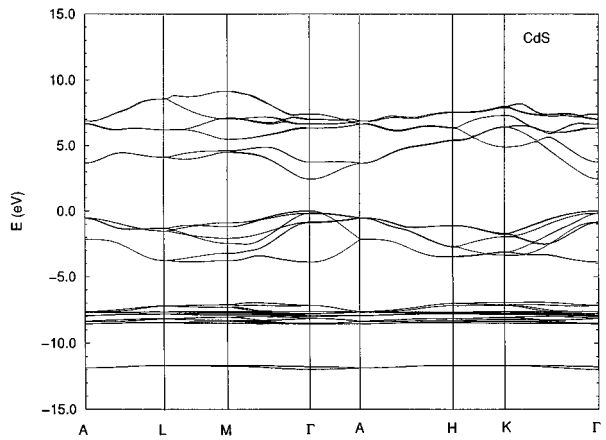

FIG. 5. Band structure calculated for wurtzite CdS using the LMTO (band-gap adjusted LDA version). The valence-band maximum has been placed at the zero of the energy scale.

TABLE IV. Calculated Γ-point energies (E_u and E_a, in eV) and linear spin-splitting coefficients (C_u and C_a, in meV Å, *magnitude only*; for the signs, see text) for the e, Γ_{9v}, Γ_{7v}, and $\Gamma_{7'v}$ edges of wurtzite CdS, CdSe, and ZnO obtained from band-gap unadjusted (u) and adjusted (a) ASA-LMTO calculations. The lattice parameters used are from Table III, except for the unadjusted ZnO data for which ideal c/a and u values were used. Also tabulated are ratios of unadjusted and adjusted gaps: $g=E_7-E_{7'}$, $G=E_e-E_5$, where $E_5=(E_7+E_{7'})/2$.

C_u	E_u		E_a	C_a	C_u/C_a	g_u/g_a	G_u/G_a
CdS:							
36.8	1.12	e	2.43	11.7	3.1		
							1/2.1
182	0	7	0	82	2.2		
—	0.076	9	0.153	—		1/1.6	
100	0.118	7′	0.194	26.5	3.8		
CdSe:							
675	0.38	e	1.83	59.5	11.3		
							1/3.5
1100	0	7	0	192	5.7		
—	0.050	9	0.120	—		1/1.14	
450	0.427	7′	0.480	95	4.7		
ZnO:							
9.0	1.08	e	3.36	1.1	8.2		
							1/3.2
120	0	7	0	6.3	19		
175	0.038	7′	0.200	58	3	1/5.1	
—	0.043	9	0.220	—			

III. LMTO CALCULATIONS

A. Procedure

The electronic band structures are calculated within the framework of density-functional theory using the local-density approximation (LDA) within the atomic-sphere approximation (ASA), including the so-called "combined-correction term."[40] The spin-orbit interaction is treated as a perturbation.[41] Each unit cell consists of eight "atoms," including four "empty spheres" with no net nuclear charge, positioned in the empty tetrahedral sites in order to obtain a close-packed structure.[42] Wave functions in all eight spheres (atomic and empty) are expressed in terms of s, p, and d partial waves resulting in a Hamiltonian matrix of dimension 144 (8 atoms $\times$ 9 partial waves $\times$ 2 spin states).

Adjusting potentials can be located at the atomic and empty spheres in order to correct for the so-called "gap problem" inherent in the LDA formalism.[43] In this way, the band gaps can be brought into agreement with experimental results. The resulting effective masses are expected to be correct, since wave functions are not strongly affected by the adjusting potentials, thus simulating the effect of quasiparticle corrections in the GW approximation.[44,45] We use δ-function-like adjusting potentials of the form

$$V(r)=V_0\frac{R_0}{r}\exp\left[-\frac{r^2}{R_0^2}\right]. \tag{25}$$

Table II gives the potential parameters used for CdS. The atomic-sphere radius is set equal for cations and anions for simplicity.

Beside the atomic-sphere radii, related to the primitive-cell volume, additional variables are present in our calculations: the c/a ratio and the bond-length parameter u of a wurtzite crystal. A hard-sphere model of hexagonal closed-packed and touching atoms gives an ideal c/a ratio of $\sqrt{8/3}=1.633$. In addition, the assumption of equal nearest-neighbor bond lengths for the wurtzite crystal leads to the ''ideal value''

$$u=\frac{1}{3}\left(\frac{a}{c}\right)^2+\frac{1}{4}. \tag{26}$$

The band edges are found to be somewhat dependent upon the c/a ratio but less so upon u, since the crystal-field interaction is more strongly dependent on the c/a ratio and u is only related to the nearest-neighbor environment. We have used experimental values of the lattice parameters a and c given in Table III. The calculations were performed using ideal u values; the latter agree well with available experimental data (Table III). In fact, the ideal u's are closer to the experimental values than those obtained using the total-energy full-potential LMTO method and the experimental equilibrium volume (Table III). We will also present some results obtained using the ideal c/a ratio for ZnO.

B. Band structure

In Fig. 5 we show the band structure of CdS obtained by the LMTO method. The lowest gap of CdS is direct and is found experimentally to be 2.58 eV at low temperature. We have carried out potential adjusted and unadjusted calculations. Previous empirical evaluations of the band structure, including tight-binding[46] and pseudopotential calculations,[47] do not include spin-orbit interaction. Furthermore, the tight-binding calculations do not include d states. There are some recent *ab initio* calculations, again without spin-orbit interaction but with d orbitals, based upon Gaussian orbitals.[48,49]

Our LMTO calculations were performed using the atomic-sphere approximation. One estimates the resulting accuracy of the band energies to be around 100 meV. This does, in fact, lead to a minor complication with regard to the relative position of the A, B, and C holes. For instance, for CdS, the experimental E_A-E_B separation is 16 meV.[50] As such, our calculations within the ASA lead to an incorrect Γ_7, Γ_9, and $\Gamma_{7'}$ ordering for the A, B, and C states, respectively, for CdS and CdSe. For ZnO, we obtain the (also incorrect) Γ_7, $\Gamma_{7'}$, and Γ_9 ordering. In Table IV, we present the calculated band-edge energies with (E_a) and without (E_u) band-gap adjustment. Even in the adjusted case, the valence-band energies are poorly reproduced (compare with the experimental values in Table V). The ordering problem can only be corrected by making use of the much more complicated full-potential LMTO method.[51] Indeed, we have compared a band-structure calculation for CdS with experimental values of a and c using the ASA and scalar-relativistic full-potential LMTO (our full-potential program does not include spin-orbit splittings). We obtained $E(\Gamma_1)>E(\Gamma_5)$ in the ASA case, $E(\Gamma_5)>E(\Gamma_1)$ in the full-potential case.

TABLE V. Experimental Γ-point energies for the e, A, B, and C edges of wurtzite CdS, CdSe, and ZnO. Only the magnitude of the energy separation from the A energy is given.

	CdS	CdSe	ZnO
E_e	2.583 [a]	1.829 [b]	3.44 [c]
E_A	0	0	0
E_B	0.016 [a]	0.026 [b]	0.0024 [c]
E_C	0.078 [a]	0.429 [b]	0.0404 [c]

[a] $T=1.6$–4.2 K, Ref. 50.

[b] $T=80$ K, exciton reflectance, V. V. Sobolev, V. I. Donetskikh, and E. F. Zagaĭnov, Sov. Phys. Semicond. **12**, 646 (1978).

[c] $T=6$ K, two-photon spectroscopy, A. Mang, K. Reimann, and S. Rübenacke, Solid State Commun. **94**, 251 (1995).

The calculations allow one to extract the contribution of the various angular-momentum components to the eigenstates. These are given in Table VI for CdS and ZnO (the data for CdSe are very similar to those for CdS). This knowledge has been used in differentiating among the Γ_9, Γ_7, and $\Gamma_{7'}$ states: The Γ_7 states should contain larger s-like compo-

TABLE VI. Angular-momentum (l) decomposition of C', B', A', and e states for each type of atom as calculated with the ASA-LMTO method. The primes are to remind one that the relative ordering of the states is different from the experimental one. The data for CdSe are very similar to those for CdS and hence are not displayed. The tabulated numbers are the magnitude squared of the wave functions. $E1$ and $E2$ denote empty spheres.

		C'	B'	A'	e
CdS:					
Cd	$l=0$	0.0000	0.0000	0.0001	0.2993
	$l=1$	0.0348	0.0311	0.0363	0.0000
	$l=2$	0.1182	0.1104	0.1107	0.0007
S	$l=0$	0.0000	0.0000	0.0000	0.2282
	$l=1$	0.8053	0.8150	0.7717	0.0010
	$l=2$	0.0001	0.0001	0.0003	0.0005
$E1$	$l=0$	0.0004	0.0000	0.0142	0.0809
	$l=1$	0.0003	0.0000	0.0166	0.0081
	$l=2$	0.0083	0.0080	0.0227	0.0018
$E2$	$l=0$	0.0002	0.0000	0.0059	0.3657
	$l=1$	0.0174	0.0204	0.0082	0.0096
	$l=2$	0.0150	0.0149	0.0132	0.0043
ZnO:					
Zn	$l=0$	0.0000	0.0000	0.0007	0.2533
	$l=1$	0.0129	0.0133	0.0172	0.0002
	$l=2$	0.2601	0.2684	0.2480	0.0045
O	$l=0$	0.0000	0.0000	0.0005	0.1904
	$l=1$	0.7083	0.7001	0.6881	0.0004
	$l=2$	0.0003	0.0003	0.0002	0.0002
$E1$	$l=0$	0.0000	0.0000	0.0087	0.0993
	$l=1$	0.0000	0.0001	0.0060	0.0044
	$l=2$	0.0028	0.0028	0.0160	0.0014
$E2$	$l=0$	0.0000	0.0000	0.0090	0.4357
	$l=1$	0.0062	0.0054	0.0022	0.0054
	$l=2$	0.0093	0.0095	0.0033	0.0050

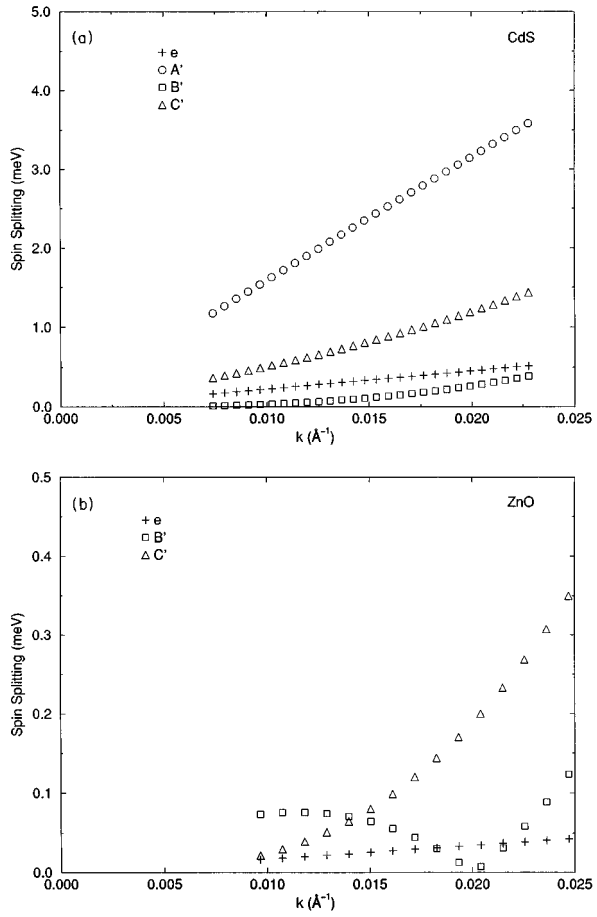

FIG. 6. Spin splitting (magnitude only) of the first conduction state e, and the top three valence states A', B', and C' away from the Γ point along the $\Gamma-K$ direction. (a) For CdS. (b) For ZnO (here A' is not included since it is offscale). These results were obtained from unadjusted *ab initio* ASA-LMTO calculations.

nents. One interesting result is that all of the A', B', and C' states (where the primes denote the LMTO ordering) have around 11% Cd d composition for CdS and CdSe, and around 26% Zn d for ZnO. The increase for ZnO compared to the Cd compounds is due to the Zn d state being closer to the valence-band top ($\sim$4 eV) than the Cd d state ($\sim$8 eV). This is in agreement with the nonrelativistic *ab initio* calculations of Schröer *et al.*[48,49]

C. Spin splittings

The question of whether one can extract reliable spin splittings from the band-structure calculations performed within LDA and ASA cannot be answered alone from our LMTO results. However, we will show that the calculation can be rescued from deficiencies related to the errors in the valence-band energies by using the understanding of how the C_i's depend on the band energies determined with our $\mathbf{k}\cdot\mathbf{p}$ analysis.

We have, therefore, computed the linear spin-splitting coefficients using both band-gap adjusted and unadjusted band structures. The spin-splitting energies (magnitude only) calculated along Γ-K for CdS and ZnO are plotted in Fig. 6. The calculated points start at a nonzero value of the wave vector due to numerical problems of the LDA code for $k\rightarrow 0$. By fitting the separation of the split-band energies with

$$|\Delta E_i(k)| = 2C_i k + \gamma_i k^3, \tag{27}$$

we obtain the spin-splitting coefficients C_i and γ_i and their relative sign. We have included both the linear and cubic terms in Eq. (27): The corresponding C_i's are given in Table IV. It is clear that they depend on the band gap.

We now analyze the calculated C_i's with the help of Eq. (24). As a preliminary step, we have calculated the spin-orbit (Δ_{so}) and crystal-field (Δ_{cf}) energies using the quasicubic expressions:

$$\left.\begin{matrix}\Delta_{cf}\\ \Delta_{so}\end{matrix}\right\} = \frac{1}{2}[\Delta_{CB}-\Delta_{BA}\pm\sqrt{2\Delta_{CA}^2-\Delta_{BA}^2-\Delta_{CB}^2}], \tag{28}$$

with $\Delta_{CB}=E_C-E_B$, etc. Good agreement of the Δ_{so} obtained from both adjusted *and* unadjusted LMTO calculations, and also experimentally, is found for CdS and CdSe (Table VII). As for ZnO, a relatively good Δ_{so} is obtained with no adjusting potentials and ideal lattice parameters. However, such agreement is not found when using adjusting potentials; the data displayed in Table VII for the adjusted case were obtained using experimental lattice parameters. In the case of ZnO, Δ_{so} is very sensitive to the potential and lattice parameters because of the opposite sign of the atomic spin-orbit energies of Zn and O, which partly compensate each other and lead to the negative value of Δ_{so} (the Zn $3d$ splitting dominates). The disagreement between theory and experiment for Δ_{cf} in all materials again reflects the shortcoming of the ASA and also the errors of $\approx$0.1 eV expected for any state-of-the-art band-structure calculations. An important result is that, in employing Eq. (24), the spin-orbit matrix elements can be assumed to be energy independent (for CdS and CdSe). The interband momentum matrix elements are also known to be unaffected by the band-gap problem.[44,45] Hence, we analyze the C_i's in terms of the corresponding energy denominators.

TABLE VII. Crystal-field (Δ_{cf}) and spin-orbit (Δ_{so}) energies (in meV) for CdS, CdSe, and ZnO as evaluated from the data in Table IV by using Eq. (28). The first number for each quantity is the one obtained without adjusting potentials, the second one with adjusting potentials. In brackets are the experimental values (Ref. 50).

	CdS	CdSe	ZnO
Δ_{cf}	-88, -168 (30)	-89, -161 (39)	-40, -208 (188)
Δ_{so}	54, 56 (65)	396, 401 (416)	-7, -32 (-3.5)

In Table IV we have included the ratio of unadjusted and adjusted energies for two gaps: $E_7-E_{7'}$ and E_e-E_5 [E_5 being an average valence energy, here chosen as $(E_7+E_{7'})/2$]. It can be inferred that, for all three materials, C_e follows the inverse-square-of-the-average-gap relation. Similarly, $C_{7'}$ of CdS, and C_7 and $C_{7'}$ of CdSe display the energy dependence of the $\mathscr{B}$ term of Eq. (24). Hence, the $\mathscr{B}$-dependent contribution is dominant. C_7 of CdS, however, scales better with just the E_e-E_5 gap. Since Δ_{so} has changed drastically for ZnO, no such deductions can be arrived at. Given the above scaling rules (which we will also

TABLE VIII. Linear-spin-splitting coefficient C_i (in meV Å) of the band edge of wurtzite CdS, CdSe, and ZnO. The ''theory'' values were obtained using *ab initio* ASA-LMTO. Note that the valence C_i have been renormalized to correct for ''gap problems'' (compare Table IV). In all cases, absolute values of the splittings are listed (see text for information on the signs). The data in italics have been derived from the experimental excitonic coefficients given in Table X and the effective masses from Table IX.

		CdS	CdSe	ZnO
C_e	theory	12	60	1.1
	expt.	16[a], *8*[b], *11*[c]	<100[g]	—
C_A	theory	0	0	35
	expt.	0	0	20[h]
C_B	theory	82[d], 246[e]	230	0
	expt.	*67*[f]	<900[g]	0
C_C	theory	70	114	51

[a]Spin-flip Raman scattering, Ref. 3.
[b]Calculated from ϕ_A of Ref. 28 (see Table X).
[c]Calculated from ϕ_A of Ref. 30 (see Table X).
[d]Assuming $C_B \propto (E_e - E_5)^{-1}$.
[e]Assuming $C_B \propto (E_e - E_5)(E_7 - E_{7'})^{-1}$.
[f]Calculated by Koteles and Winterling (Ref. 24) from their ϕ_B (see Table X).
[g]Estimates from Ref. 19.
[h]Assuming $C_e = 0$. Magnetoluminescence, Ref. 22; reflection, transmission, and two-photon Raman scattering, Ref. 27.

assume valid for ZnO), we renormalize the directly computed C_i's to reflect the correct energy gaps. Since our adjusted calculations reproduce reasonably well the experimental E_0 gaps, we have only renormalized the valence C_i's. The renormalized C_i's are displayed in Table VIII together with experimental values. For C_7 of CdS, we have renormalized it with respect to the $E_e - E_5$ gap (giving $C_B = 82$ meV Å) and to the $(E_e - E_5)$ and $(E_7 - E_{7'})$ gaps (giving $C_B = 246$ meV Å). The renormalization with respect to only the $E_e - E_5$ gap gives a much better agreement with the experimental result. Hopfield[19] had also given upper bounds for C_e of CdS and CdSe (10 and 20 meV Å, respectively) from an analysis of Zeeman-splitting experiments. While this compares reasonably well with other results for CdS (Table VIII), it is much smaller than our calculated value in the case of CdSe.

We have also made an attempt to compute the individual contributions (magnitude and sign) to the C_i's by combining the unadjusted and adjusted LMTO results with the $\mathbf{k}\cdot\mathbf{p}$ analysis in the cases of CdS and CdSe. Using values for q_7 from the literature[38] ($q_7^2 = 0.31$ for CdS and $q_7^2 = 0.6$ for CdSe), we computed $\mathscr{A}$ using the expression for C_e in Eq. (24). $C_{7,e}$ and $C_{7',e}$ are subsequently determined. The remaining contribution to C_7 can then be found from the total C_7 obtained in the LMTO calculation. Since the remaining contribution to $C_{7'}$ is just the opposite in sign, this can be used to calculate $C_{7'}$. A comparison of the latter with the LMTO-calculated value provides a clue as to the overall correctness of the procedure and Eq. (24). This was done for the unadjusted (u) and adjusted (a) data from LMTO, and the results (best fit, see below) are as follows:

	CdS (u)	CdS (a)	CdSe (u)	CdSe (a)
$C_{7'}$ ($\mathbf{k}\cdot\mathbf{p}$ +LMTO)	+145	+70	+425	+133
$C_{7'}$ (LMTO)	100	27	450	95
$C_{7,7'}/C_{7,e}$ (approx.)	+5	+9	+2	+6

While the agreement between the first two rows of the above table is not perfect, it is reasonable in view of the semiquantitative aspect of this analysis. Note that the best agreement was obtained for

$$C_7 < 0, \quad C_{7'} > 0. \tag{29}$$

It is gratifying to find $|C_{7,7'}| > |C_{7,e}|$, as expected [see Eq. (23)].

In order to compare with the zinc-blende-type semiconductors, we have also calculated the spin splitting for cubic CdSe. For example, $C_B = 230$ meV Å found for wurtzite CdSe must be compared with $|C_k| = 46$ meV Å for zinc-blende CdSe (found using band-gap adjusted ASA-LMTO). A good estimate of the zinc-blende coefficient is given by the following expression:[10]

$$C_k = -A\frac{\Delta_{d,c}}{E(\Gamma_8) - E_{d,c}} + B\frac{\Delta_{d,a}}{E(\Gamma_8) - E_{d,a}}, \tag{30}$$

where $\Delta_{d,c}$ ($\Delta_{d,a}$) is the spin-orbit splitting of the core d levels of the cation (anion), $E_{d,c}$ ($E_{d,a}$) their energy, and $A = 350$ meV Å and $B = 90$ meV Å for II-VI compounds. Using the data provided in Table I of Ref. 10 and $E(\Gamma_8) - E_{d,c} \approx 8$ eV (from our present LMTO calculation), we obtain $C_k = -33$ meV Å, in reasonable agreement with the LMTO result. We also predict that cubic CdS would have a C_k very close to that of CdSe while the C_i's differ significantly in the wurtzite structure (Table VIII). In general, one expects larger linear spin splittings for wurtzite semiconductors because they are mainly determined by the $\Gamma_{7c} - \Gamma_{7v}$ and $\Gamma_{7v} - \Gamma_{7'v}$ gaps instead of the gap to the d electrons for zinc-blende. Cancellation effects among the three terms in C_7 can reduce them below the corresponding zinc-blende coefficient. Nevertheless, this does not occur for CdSe due to the dominance of the $\mathscr{B}$ term in Eq. (24). The hexagonal crystal field thus has a major role in enhancing the C_i's.

In exciton reflectivity and resonant Brillouin scattering experiments, one actually measures directly the linear-in-k splitting of the *exciton* dispersion (coefficient ϕ_i, with i representing the valence state). In terms of an electron (e) and a hole (h) state, ϕ_h is related to the C_i's of the electron and *hole* dispersions through the *positive* band-edge masses:

$$\phi_h = \frac{C_h m_h^{\perp} + C_e m_e^{\perp}}{m_h^{\perp} + m_e^{\perp}}. \tag{31}$$

Only the perpendicular effective masses appear since $\mathbf{k} \perp \mathbf{c}$. However, the LMTO and $\mathbf{k}\cdot\mathbf{p}$ calculations result in the linear spin-splitting coefficient of the valence electron C_v (with $v = 7$ or $7'$), so that $C_h = -C_v$. Hence, we can rewrite Eq. (31) as

TABLE IX. Band-edge effective masses for wurtzite CdS, CdSe, and ZnO.

	CdS	CdSe	ZnO
$m_\perp(e)$	0.21[a]	0.13[c]	0.275[d]
$m_\perp(A)$	0.68[a]	0.45[c]	0.59[e]
$m_{\|\|}(A)$		>1[c]	0.59[e]
$m_\perp(B)$	0.64[b]	0.9[c]	0.59[e]
$m_{\|\|}(B)$			0.59[e]
$m_\perp(C)$	>1[f]	>1[f]	0.31[e]
$m_{\|\|}(C)$	>1[f]	>1[f]	0.55[e]

[a]Resonant Brillouin scattering, Ref. 30.
[b]Two-photon spectroscopy, D. G. Seiler, D. Heiman, and B. S. Wherrett, Phys. Rev. B **27**, 2355 (1983).
[c]Zeeman splitting of excitons, R. G. Wheeler and J. O. Dimmock, Phys. Rev. **125**, 1805 (1962).
[d]Cyclotron resonance, K. J. Button, D. R. Cohn, M. von Ortenbert, B. Lax, E. Mollwo, and R. Helbig, Phys. Rev. Lett. **28**, 1637 (1972).
[e]Reference 50.
[f]Present work. Estimates based on $\mathbf{k}\cdot\mathbf{p}$ analysis and LMTO band structures.

$$\phi_h=\frac{-C_v m_h^\perp + C_e m_e^\perp}{m_h^\perp + m_e^\perp}. \tag{32}$$

There is a sign difference between Eq. (32) above and Eq. (1) of Ref. 24 where, however, the authors were not concerned with the sign of ϕ_i. Here, we have for CdS, $C_e>0$, $C_B<0$. The ϕ_i's obtained from the calculated C_i's and the effective masses given in Table IX are tabulated in Table X.

For completeness, it is interesting to note that an infinite number of invariants can be constructed by simply taking higher powers of the linear-k invariant [Eq. (3)]:

$$[k_x\sigma_y - k_y\sigma_x]^{2n+1} = k_{||}^{2n}[k_x\sigma_y - k_y\sigma_x], \tag{33}$$

where $k_{||}$ is the magnitude of the in-plane wave vector and n is a positive integer. If these were the only invariants, then the in-plane spin splittings would be isotropic. We find this to be well-obeyed for small $k_{||}$, but to break down for larger $k_{||}$ (typically >0.2 Å^{-1}).

IV. CONCLUSION

We have presented a microscopic calculation of the linear spin-splitting coefficients for the e, A, B, and C states of CdS, CdSe, and ZnO with the wurtzite structure. Their origins have been analyzed using the $\mathbf{k}\cdot\mathbf{p}$ model and are shown to be quite different from the zinc-blende case. Our work reveals the limitation of state-of-the-art band-structure calculations in reproducing the correct hexagonal crystal-field energies. Therefore, a renormalization of the valence C_i's was found necessary. We warn that band parameter calculations which do not correct for errors in the calculated band energies, in particular those reported in Ref. 52 for the valence bands of wurtzitelike AlN and GaN, should be treated with caution.

The calculated and renormalized C_e and C_B for CdS and C_A for ZnO are in good agreement with the corresponding experimental values. The small calculated C_e for ZnO justifies the approximation $C_e\approx 0$ used in experimental A-exciton work. The calculated C_e and C_B for CdSe are consistent with theoretical upper-bound values obtained previously.[19]

For CdS and CdSe, with $C_e>0$, we predict $C_B<0$, $C_C>0$; in addition, $|C_B|>|C_C|$. An important experiment would be to confirm that C_e for CdSe is much larger than the upper-bound value of 20 meV Å deduced from Zeeman-splitting experiments.[19,34] For ZnO, we predict $|C_C|>|C_A|$. It would be interesting to determine experimentally the sign of C_e for ZnO and the Cd compounds. Due to the comparable magnitude of the linear spin splitting of the excitons for CdS and CdSe to those of the copper halides (for which $C_k\sim 60$ meV Å),[6,31] we expect the linear spin-splitting terms to be directly observable in luminescence experiments on CdS and CdSe microcrystallites or quantum dots, as was reported for copper halide microcrystallites.[6]

TABLE X. Exciton linear-spin-splitting coefficient (in meV Å) for wurtzite CdS, CdSe, and ZnO. In all cases, absolute values of the splittings are given (see text for information on the signs). The data in italics have been derived from the experimental band coefficients C_i given in Table VIII and the effective masses from Table IX.

		CdS	CdSe	ZnO
ϕ_A	theory	2.7	13	24
	expt.	1.9[a], 2.7[b], *3.8*[c]	—	*14*[g]
ϕ_B	theory	65, 188	209	0
	expt.	40[d], 56 ± 4[e], 60[f]	—	—
ϕ_C	theory	70[h]	114[h]	28

[a]Resonant Brillouin scattering, Ref. 28.
[b]Resonant Brillouin scattering, Ref. 30.
[c]Calculated in Ref. 28 from data of Ref. 3 (see Table VIII).
[d]Reflection, transmission, and two-photon Raman scattering, Ref. 27.
[e]Resonant Brillouin scattering, Ref. 24.
[f]Reflectivity, Ref. 23.
[g]Magnetoluminescence, Ref. 22; reflection, transmission, and two-photon Raman scattering, Ref. 27.
[h]Assuming $|\phi_C|\approx|C_C|$.

ACKNOWLEDGMENTS

We thank the Fonds der Chemischen Industrie for partial support and T. L. Reinecke for a critical reading of the manuscript. L.C.L.Y.V. thanks the Alexander von Humboldt Foundation for financial support. M.W. acknowledges financial support from the Danish Natural Science Research Council.

APPENDIX

Here we summarize general formulas for the contribution to the linear spin-splitting coefficients which arise in second-order perturbation theory. The amount of work is reduced considerably by recognizing that

$$\langle jm|H_2|jm'\rangle = \delta_{mm'}.$$

The second-order contribution for the e state interacting with $\overline{\Gamma}_7$ and $\overline{\Gamma}_{7'}$ states is

$$C_{e,2}\equiv\sum_{\overline{7}} C_{e,\overline{7}}+\sum_{\overline{7'}} C_{e,\overline{7'}}, \tag{A1}$$

with

$$C_{e,\overline{7}}=(1-\overline{q_7^2})\frac{\Delta_{\overline{x},z}}{E_e-E_7}P_{\overline{x},S}, \tag{A2}$$

$$C_{e,\overline{7'}}=\overline{q_7'}\frac{\Delta_{\overline{x},z}}{E_e-E_{7'}}P_{\overline{x},S}, \tag{A3}$$

and

$$\Delta_{\overline{x},z}=\frac{\hbar^2}{2m_0^3c^2}\langle\overline{x}|\nabla_z Vp_x-\nabla_x Vp_z|z\rangle, \tag{A4}$$

$$P_{\overline{x},S}=-i\hbar\langle\overline{x}|\frac{\partial}{\partial x}|S\rangle. \tag{A5}$$

We now consider the valence states. If we include all possible $\overline{\Gamma_7}$ and $\overline{\Gamma_{7'}}$ states of the types from Eq. (10), and the s-like Γ_7 states, then

$$C_{7,2}\equiv C_{7,e}+\sum_{\overline{7}} C_{7,\overline{7}}+\sum_{\overline{7'}} C_{7,\overline{7'}}, \tag{A6}$$

$$C_{7',2}\equiv C_{7',e}+\sum_{\overline{7}} C_{7',\overline{7}}+\sum_{\overline{7'}} C_{7',\overline{7}}, \tag{A7}$$

with

$$C_{7,e}=(1-q_7^2)\frac{q_z\Delta_{x,z}}{E_7-E_e}P_{x,S},$$

$$C_{7,\overline{7}}=\frac{\Delta^7_{1\overline{1}}}{\sqrt{2}(E_7-\overline{E_7})}[\overline{q_7}(1-q_7^2)^{1/2}P_{x,\overline{Z}}+q_7(1-\overline{q_7^2})^{1/2}P_{Z,\overline{x}}],$$

$$C_{7,\overline{7'}}=\frac{\Delta^7_{1\overline{1'}}}{\sqrt{2}(E_7-\overline{E_{7'}})}[+(1-q_7^2)^{1/2}(1-\overline{q_7^2})^{1/2}P_{x,\overline{Z}}-q_7\overline{q_7}P_{Z,\overline{x}}],$$

$$C_{7',e}=q_7^2\frac{q_z\Delta_{x,z}}{E_{7'}-E_e}P_{x,S}, \tag{A8}$$

$$C_{7',\overline{7}}=\frac{\Delta^7_{1'\overline{1}}}{\sqrt{2}(E_{7'}-\overline{E_7})}[-q_7\overline{q_7}P_{x,\overline{Z}}+(1-q_7^2)^{1/2}\times(1-\overline{q_7^2})^{1/2}P_{Z,\overline{x}}],$$

$$C_{7',\overline{7'}}=\frac{\Delta^7_{1'\overline{1'}}}{\sqrt{2}(E_{7'}-\overline{E_{7'}})}[-q_7(1-\overline{q_7^2})^{1/2}P_{x,\overline{Z}}-\overline{q_7}(1-q_7^2)^{1/2}P_{Z,\overline{x}}],$$

where

$$\Delta^7_{1\overline{1}}\equiv\langle\Gamma_7\uparrow|H_2|\overline{\Gamma_7}\uparrow\rangle=-(1-q_7^2)^{1/2}(1-\overline{q_7^2})^{1/2}\Delta_5+\overline{q_7}(1-q_7^2)^{1/2}\Delta_{51}+q_7(1-\overline{q_7^2})^{1/2}\Delta_{15},$$

$$\Delta^7_{1\overline{1'}}\equiv\langle\Gamma_7\uparrow|H_2|\overline{\Gamma_{7'}}\uparrow\rangle=\overline{q_7}(1-q_7^2)^{1/2}\Delta_5+(1-q_7^2)^{1/2}\times(1-\overline{q_7^2})^{1/2}\Delta_{51}-q_7\overline{q_7}\Delta_{15},$$

$$\Delta^7_{1',\overline{1}}\equiv\langle\Gamma_{7'}\uparrow|H_2|\overline{\Gamma_7}\uparrow\rangle=q_7(1-\overline{q_7^2})^{1/2}\Delta_5-q_7\overline{q_7}\Delta_{51}+(1-q_7^2)^{1/2}(1-\overline{q_7^2})^{1/2}\Delta_{15}, \tag{A9}$$

$$\Delta^7_{1',\overline{1'}}\equiv\langle\Gamma_{7'}\uparrow|H_2|\overline{\Gamma_{7'}}\uparrow\rangle=-q_7\overline{q_7}\Delta_5-q_7(1-\overline{q_7^2})^{1/2}\Delta_{51}-\overline{q_7}(1-q_7^2)^{1/2}\Delta_{15},$$

and

$$\Delta_5\equiv\langle u_5\uparrow|H_2|\overline{u_5}\uparrow\rangle=\frac{-\hbar^2}{2m_0^3c^2}\left\langle x\left|\frac{\partial V}{\partial x}p_y-\frac{\partial V}{\partial y}p_x\right|\overline{y}\right\rangle,$$

$$\Delta_{51}\equiv\langle u_5^*\uparrow|H_2|\overline{u_1}\downarrow\rangle=\frac{\hbar^2}{\sqrt{2}m_0^3c^2}\left\langle x\left|\frac{\partial V}{\partial z}p_x-\frac{\partial V}{\partial x}p_z\right|\overline{Z}\right\rangle, \tag{A10}$$

$$\Delta_{15}\equiv\langle u_1\downarrow|H_2|\overline{u_5^*}\uparrow\rangle=-\frac{\hbar^2}{\sqrt{2}m_0^3c^2}\left\langle Z\left|\frac{\partial V}{\partial z}p_x-\frac{\partial V}{\partial x}p_z\right|\overline{x}\right\rangle,$$

are spin-orbit matrix elements. $P_{x,\overline{Z}}=-i\hbar\langle x|\partial/\partial x|\overline{Z}\rangle$ (and similarly for the other momentum matrix elements).

[1] G. Dresselhaus, Phys. Rev. **100**, 580 (1955).
[2] R. C. Casella, Phys. Rev. **114**, 1514 (1959).
[3] R. Romestain, S. Geschwind, and G. E. Devlin, Phys. Rev. Lett. **39**, 1583 (1977).
[4] M. I. D'yakonov, V. A. Marushchak, V. I. Perel', and A. N. Titkov, Zh. Éksp. Teor. Fiz. **90**, 1123 (1986) [Sov. Phys. JETP **63**, 655 (1986)].
[5] H. Riechert, S. F. Alvarado, A. N. Titkov, and V. I. Safarov, Phys. Rev. Lett. **52**, 2297 (1984).
[6] T. Itoh, Y. Iwabuchi, and T. Kirihara, Phys. Status Solidi B **146**, 531 (1988).
[7] P. D. Dresselhaus, C. M. A. Papavassilious, and R.G. Wheeler, Phys. Rev. Lett. **68**, 106 (1995).
[8] P. V. Santos, M. Willatzen, M. Cardona, and A. Cantarero, Phys. Rev. B **51**, 5121 (1995).
[9] B. Jusserand *et al.*, Phys. Rev. B **51**, 4707 (1995).
[10] M. Cardona, N. E. Christensen, and G. Fasol, Phys. Rev. Lett. **56**, 2831 (1986).
[11] J. L. Birman, Phys. Rev. Lett. **2**, 157 (1959).
[12] D. G. Thomas and J. J. Hopfield, Phys. Rev. **116**, 573 (1959).
[13] J. E. Rowe, M. Cardona, and F. H. Pollak, Solid State Commun. **6**, 239 (1968).
[14] G. Dresselhaus, Phys. Rev. **105**, 135 (1957).
[15] G. Dresselhaus, J. Phys. Chem. Solids **1**, 14 (1956).

[16] R. C. Casella, Phys. Rev. Lett. **5**, 371 (1960).
[17] J. J. Hopfield, J. Phys. Chem. Solids **15**, 97 (1960).
[18] J. J. Hopfield and D. G. Thomas, Phys. Rev. **122**, 35 (1961).
[19] J. J. Hopfield, J. Appl. Phys. **32**, 2277 (1961).
[20] J. J. Hopfield and D. G. Thomas, Phys. Rev. **132**, 563 (1963).
[21] G. D. Mahan and J. J. Hopfield, Phys. Rev. **135**, A428 (1964).
[22] K. Hümmer, R. Helbig, and M. Baumgärtner, Phys. Status Solidi B **86**, 527 (1978).
[23] I. Broser and M. Rosenzweig, Phys. Status Solidi B **95**, 141 (1979).
[24] E. S. Koteles and G. Winterling, Phys. Rev. Lett. **44**, 948 (1980).
[25] W. Brenig, R. Zeyher, and J. L. Birman, Phys. Rev. B **6**, 4617 (1972).
[26] S. I. Pekar, *Crystal Optics and Additional Light Waves* (Benjamin/Cummins, Menlo Park, 1983).
[27] G. Blattner, G. Kurtze, G. Schmieder, and C. Klingshirn, Phys. Rev. B **25**, 7413 (1982).
[28] T. Shigenari, X. Z. Lu, and H. Z. Cummins, Phys. Rev. B **30**, 1962 (1984).
[29] X. Z. Lu, M. Dutta, T. Shigenari, and H. Z. Cummins, Phys. Rev. B **32**, 1037 (1985).
[30] X. Z. Lu, M. Dutta, and H. Z. Cummins, Phys. Rev. B **33**, 2945 (1986).
[31] M. Cardona, N. E. Christensen, and G. Fasol, Phys. Rev. B **38**, 1806 (1988).
[32] F. J. Espinoza-Beltran and P. Halevi, Solid State Commun. **74**, 655 (1990).
[33] G. Lommer, F. Malcher, and U. Rössler, Phys. Rev. Lett. **60**, 728 (1988).
[34] For another discussion of the spin splittings in CdS, CdSe, and ZnS see K. Ohta, Phys. Rev. **184**, 721 (1969).
[35] E. O. Kane, in *Physics of III-V Compounds*, Vol. 1 of *Semiconductors and Semimetals*, edited by R. K. Willardson and A. C. Beer (Academic, New York, 1966), Chap. 3, pp. 75–100.
[36] G. F. Koster, in *Solid-State Physics*, edited by F. Seitz and D. Turnbull (Academic Press, New York, 1957), Vol. 5, pp. 173–256.
[37] E. Gutsche and E. Jahne, Phys. Status Solidi **19**, 823 (1967).
[38] C. Hermann and C. Weisbuch, Phys. Rev. B **15**, 823 (1977).
[39] M. Cardona, N. E. Christensen, M. Dobrowolska, J. K. Furdyna, and S. Rodriguez, Solid State Commun. **60**, 17 (1986).
[40] O. K. Andersen, Phys. Rev. B **12**, 3060 (1975).
[41] G. B. Bachelet and N. E. Christensen, Phys. Rev. B **31**, 879 (1985).
[42] D. Glötzel, B. Segal, and O. K. Andersen, Solid State Commun. **36**, 403 (1980).
[43] N. E. Christensen, Phys. Rev. B **30**, 5753 (1984).
[44] M. S. Hybertsen and S. G. Louie, Phys. Rev. B **34**, 5390 (1986).
[45] M. Rohlfing, P. Krüger, and J. Pollmann, Phys. Rev. B **24**, 17 791 (1993).
[46] A. Kobayashi, O. F. Sankey, S. M. Volz, and J. D. Dow, Phys. Rev. B **28**, 935 (1983).
[47] M. L. Cohen and J. R. Chelikowsky, *Electronic and Optical Properties of Semiconductors*, Springer Series in Solid-State Sciences Vol. 75 (Springer, Berlin, 1989).
[48] P. Schröer, P. Krüger, and J. Pollman, Phys. Rev. B **47**, 6971 (1993).
[49] P. Schröer, P. Krüger, and J. Pollman, Phys. Rev. B **48**, 18 264 (1993).
[50] Landolt-Börnstein, Numerical Data and Functional Relationships in Science and Technology, Vol. 22a, Group III, edited by K.-H. Hellwege (Springer-Verlag, Berlin, 1982).
[51] M. Methfessel, Phys. Rev. B **38**, 1537 (1988).
[52] M. Suzuki, T. Uenoyama, and A. Yanase, Phys. Rev. B **52**, 8132 (1995).
[53] G. F. Koster, J. O. Dimmock, R. G. Wheeler, and H. Statz, *Properties of the Thirty-Two Point Groups* (MIT, Cambridge, 1963).